

by the reactivity of the oxide ion rather than by the concentration of Co in a particular oxidation state. In any case, we note the close correlation between the catalytic activity and the oxidizing power as shown in Figure 9. Similar correlations have been observed for  $\text{La}_{1-x}\text{Sr}_x\text{MnO}_3^8$  and  $\text{La}_{2-x}\text{Sr}_x\text{NiO}_4^9$  for a more limited range of  $x$  values.

Low catalytic activity for  $x = 0-0.5$  (oxygen excess) is understandable, since the oxidizing power of the surface

is relatively low and the ability to dissociate dioxygen is also low. The catalysts with oxygen-excess compositions showed low catalytic activities also in the cases of  $\text{La}_{1-x}\text{Sr}_x\text{MnO}_3^8$  and  $\text{La}_{2-x}\text{Sr}_x\text{NiO}_4$  systems.<sup>9</sup>

**Registry No.**  $\text{La}_2\text{CoO}_{4.14}$ , 119147-29-4;  $\text{La}_{1.5}\text{Sr}_{0.5}\text{CoO}_{4.04}$ , 119147-30-7;  $\text{La}_{1.2}\text{Sr}_{0.8}\text{CoO}_{4.08}$ , 119147-31-8;  $\text{LaSrCoO}_4$ , 12200-48-5;  $\text{La}_{0.8}\text{Sr}_{1.2}\text{CoO}_4$ , 115285-39-7;  $\text{La}_{0.5}\text{Sr}_{1.5}\text{CoO}_{3.92}$ , 119147-32-9;  $\text{Sr}_2\text{CoO}_{3.68}$ , 119147-33-0;  $\text{O}_2$ , 7782-44-7;  $\text{CO}$ , 630-08-0;  $\text{Co}$ , 7440-48-4.

## Analysis of Anodic Oxide Films on Niobium

N. Magnussen,\* L. Quinones, D. C. Dufner, D. L. Cocke, and E. A. Schweikert

*Department of Chemistry, Texas A&M University, College Station, Texas 77843-3255*

B. K. Patnaik, C. V. Barros Leite, and G. B. Baptista

*Departamento de Fisica, Pontificia Universidade Catolica, Rio de Janeiro, Brazil*

*Received August 31, 1988*

Anodic oxide films were grown on niobium in the presence of sodium tungstate. Two sample sets were grown at varying temperatures, and one set was grown to varying terminal voltages. The resulting films were examined by X-ray photoelectron spectroscopy (XPS) and Rutherford backscattering spectrometry (RBS). The XPS results show a close association of the sodium and tungstate species at the surface. Depth profiling shows the reduction of niobium oxide and the steady decrease in the amount of incorporated sodium with increased depth. The RBS data show multiple, overlapping peaks in the tungsten region. The layered structure is voltage dependent.

### Introduction

Anodic oxide films are important in many applications, particularly in the area of electronic and dielectric materials. The function of the anodic film can be seriously affected by the incorporation of anions during the growth process. Recent evidence shows that the presence of foreign anions may inhibit the growth of grain boundaries and increase dielectric strength.<sup>1,2</sup> The incorporation of anions into anodic oxide films has been studied for several metal/metal oxide systems.<sup>3-6</sup> However, to date, the characterization of the niobium system has received little attention.

The surface properties of niobium are also of particular technological significance because of their impact within the field of superconducting materials. It has been determined that niobium has the highest superconducting transition temperature (9.3 K) of all the elements and also the highest transition temperature for the binary compounds, with  $\text{Nb}_3\text{Ge}$  at 23 K.<sup>7</sup> Of particular importance is the use of niobium for applications in superconducting ratio frequency (rf) cavities. Performance of the rf cavities is highly dependent on the surface properties of the material used. It has been suggested that anodic oxidation of the niobium surface may be one method of improving the quality of these superconducting materials.<sup>8,9</sup> The

anodic film provides a suitable coating for the rf cavities by forming a protective, amorphous  $\text{Nb}_2\text{O}_5$  oxide overlayer, displacing the cavity surface to a purer region within the film. Preparation techniques are critical in this matter because a few angstroms difference in oxide thickness or the presence of impurities can result in large changes in the dielectric properties and, thus, drastically affect the capabilities of the material.

The present study will consider the surface and bulk characteristics of anodic oxide films grown on a niobium substrate in the presence of tungstate anion. Tungstate was a practical choice to optimize the peak separation of the substrate (low molecular weight) and the dopant (high molecular weight) for bulk analysis in Rutherford backscattering spectrometry. The effect of temperature and voltage variations on anion incorporation will be examined through the use of X-ray photoelectron spectroscopy (XPS) and Rutherford backscattering spectrometry (RBS).

XPS is an important analytical technique for surface characterization. This technique provides information regarding the binding energies of core electrons in atoms and molecules. With this information it is possible to determine what species are at the surface and, in many cases, their oxidation state. RBS, used in the low-megaelectronvolt energy range, is a powerful technique for nondestructive depth-profiling studies. This technique can be used to determine several parameters important in the study of anodic film formation. These parameters include oxide layer thickness, stoichiometric composition, and concentration and location of the incorporated film dopants. Through the use of these two techniques, we have studied the surface and bulk characteristics of the niobium anodic oxide films, and these results are presented.

(1) Thompson, G. E.; Wood, G. C.; Shimizu, K. *Electrochim. Acta.* **1981**, *26*, 951.

(2) Shimizu, K.; Thompson, G. E.; Wood, G. C. *Thin Solid Films* **1981**, *81*, 39.

(3) Skeldon, P.; Shimizu, K.; Thompson, G. E.; Wood, G. C. *Thin Solid Films* **1985**, *123*, 127.

(4) Abd Rabbo, M. F.; Richardson, J. A.; Wood, G. C. *Corros. Sci.* **1976**, *16*, 689.

(5) Konno, H.; Kobayashi, S.; Takahashi, H.; Nagayama, M. *Electrochim. Acta.* **1980**, *25*, 1667.

(6) Sharp, D. J.; Panitz, J. K. G.; Merrill, R. M.; Haaland, D. M. *Thin Solid Films* **1984**, *111*, 227.

(7) Gavler, J. R. *Appl. Phys. Lett.* **1973**, *23*, 480.

(8) Halama, H. J. *Part. Accel.* **1977**, *2*, 335.

(9) Martens, H.; Diepers, H.; Sun, R. K. *Phys. Lett.* **1971**, *34A*, 439.

### Experimental Details

**Sample Preparation.** Niobium metal sheets 0.254 mm thick (99.8% purity) were purchased from Aesar. Disks were cut from the sheets to give an exposed surface area of 1 cm in diameter. The disks were polished with progressively finer grades of paper, followed by polishing with diamond paste down to  $1/4\text{-}\mu\text{m}$  grit. The polished disks were rinsed, ultrasonically cleaned, and air dried. Examination of the prepared surface by scanning electron microscopy (JEOL 35CF) has shown a smooth, featureless surface. In addition, XPS shows no surface contaminants other than the presence of adventitious carbon.

Various electrolytes, with a wide range of pH, have been used for the production of anodic oxide films on niobium.<sup>10-12</sup> To ensure compatibility with our past and future studies, a solution of 0.15 M sodium borate/boric acid was chosen with an anion concentration 0.5 M sodium tungstate (Strem Chemical). All solutions were made with triply deionized water.

The polished niobium served as the anode and platinum metal as the cathode in the electrochemical experiment. Nitrogen gas was bubbled through the solution before and during the growth process to deoxygenate the solution and to prevent localized heating. Power was supplied by a dc power source (Hewlett Packard), and the voltage and current were monitored by digital multimeters. The temperature of the solution was maintained by an external water bath that circulated water through the outer jacket of the electrochemical cell.

Two different experiments were run—one involved varying the growth temperature while the other involved varying the terminal voltage. In the first experiment, the samples were grown to a terminal voltage of 72 V while the temperature was increased by 10 °C intervals (15 to 85 °C) for each sample. An additional sample set was grown under the same conditions, but growth was terminated at 100 V. In the second experiment, the terminal voltage was varied by 15-V intervals from 15 to 105 V while the growth temperature was held constant at 35 °C. In all experiments the current density was maintained at 10 mA/cm<sup>2</sup>. Once the terminal voltage was reached, the voltage was reduced to zero and the circuit opened. The samples were then removed from the cell, rinsed with triply deionized water, and air dried.

**Surface Analysis.** The film surfaces were analyzed by X-ray photoelectron spectroscopy (XPS) on a Kratos XSAM800 spectrometer at the Texas A&M Surface Science Center. The samples were irradiated with Mg K $\alpha$  X-rays with an energy of 1253.6 eV. Data were collected by using a DS 300 data processing system. Spectra were obtained at a typical pressure of  $2 \times 10^{-8}$  Torr. The carbon 1s peak, which is due to the presence of adsorbed carbon contaminants from the environment, was used as a reference (285.0 eV) for the binding energies. In addition, depth profiling was done on one sample, using a 5-keV argon ion beam to sputter away the surface layers. The argon pressure was maintained at  $5 \times 10^{-6}$  Torr. Periodically, etching was stopped, and XPS data were collected from the exposed subsurface layers.

**Bulk Analysis.** Identical sample sets were analyzed by Rutherford backscattering spectrometry (RBS) using a 2-MeV  $\alpha$ -particle beam generated by a Van de Graaff accelerator at the Catholic University, Rio de Janeiro, Brazil. The sample surface was irradiated by the collimated beam (0.5 mm) at normal incidence. Ions scattered at 170° were collected by using a surface barrier detector placed 12 cm from the sample. The energy resolution was determined to be 15 keV. The typical pressure in the scattering chamber was  $2 \times 10^{-6}$  Torr.

Signals were electronically amplified, and the data were acquired in a multichannel analyzer. Data smoothing routines were not used.

### Experimental Results

The first experiment involved increasing the temperature by 10 °C intervals from 15 to 85 °C, while the terminal voltage was set at 72 V. As the temperature was increased,

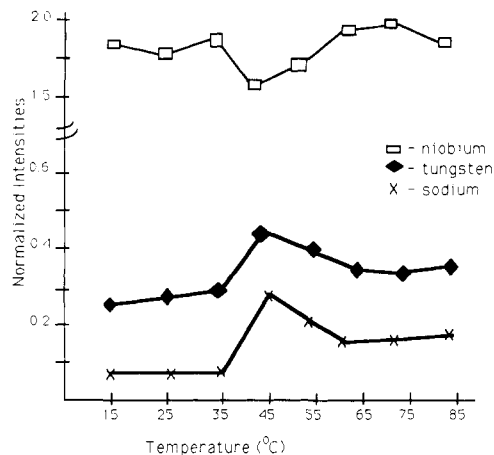


**Figure 1.** Graphed XPS data showing the trends for the niobium  $3d_{5/2}$ , tungsten  $4f_{7/2}$ , and sodium  $1s$  signals for species at the surface. Films grown at varying temperatures to a terminal voltage of 72 V.

the film color changed from red-violet to deep blue. Interference colors on anodic oxide films are well documented.<sup>13,14</sup> Although it is possible to determine film thickness through various means, for the purposes of our studies, film colors are used only as an indication of a change in relative film thickness. Given this, the observed change in film color is indicative of a slight increase in film thickness over the temperature range. No significant change in growth time was noted.

In the second sample set, the temperature was increased by 10 °C intervals from 25 to 75 °C, with a terminal voltage of 100 V. In this case the film color changed from green to rose, again indicating a slight change in thickness accompanied by no significant change in growth time over the temperature range.

In the final sample set, the temperature was maintained at 35 °C while the terminal voltage was varied between 15 and 105 V. The film color changed at each voltage, indicating a constant increase in film thickness as the voltage was increased. This is expected for barrier type films, where film thickness is dependent upon the applied voltage. The growth time also increased with the increase in terminal voltage.

**Surface Characterization of Niobium Oxide Films.** The surface characteristics of the films were examined by XPS, located at the Surface Science Center, Texas A&M University. Figures 1 and 2 show the plots of the normalized peak intensities of the surface species versus the growth temperature for the samples grown at 72 and 100 V, respectively. The close association of sodium and tungsten should be noted.

Figure 3 shows the normalized peak intensities versus the applied voltage for the samples grown at constant temperature to varying terminal voltages. Again, the sodium and tungsten species are closely associated. Additional information was collected through depth profiling on the sample grown to 30 V. Figure 4 plots the niobium ( $3d_{5/2}$ ,  $3d_{3/2}$ ) signal for the sample as received and after a 5-, 15-, and 40-min etch. In an effort to sort out the contributions of the various oxides, peak fitting was performed for the sample that was etched for 40 min. The result is shown in Figure 5, where the  $3d_{5/2}$  peak is labeled for each oxidation state. Figure 6 plots the corresponding change in the sodium  $1s$  intensity versus the etch time. It is observed that the sodium intensity decreases with in-

(10) Rigo, S.; Siejka, J. *Solid State Commun.* 1974, 15, 259.

(11) Hurlen, T.; Bentzen, H.; Hornkjøl, S. *Electrochim. Acta* 1987, 32, 1613.

(12) Torresi, R. M.; Nart, F. C. *Electrochim. Acta* 1988, 33, 1015.

(13) Vermilyea, D. A. *Acta Metall.* 1953, 1, 282.

(14) Young, L. *Anodic Oxide Films*; Academic Press: London, 1961.

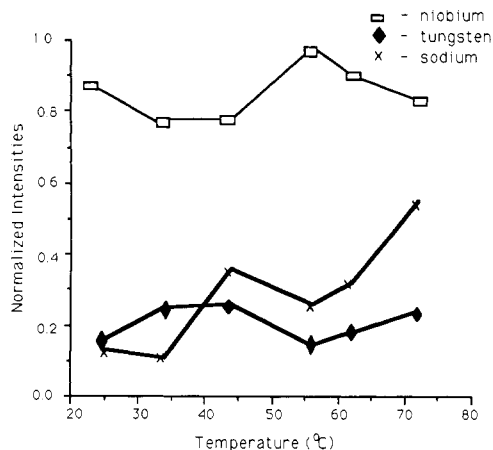


**Figure 2.** Graphed XPS data showing the trends for the niobium  $3d_{5/2}$ , tungsten  $4f_{7/2}$ , and sodium  $1s$  signals for species at the surface. Films grown at varying temperatures to a terminal voltage of 100 V.

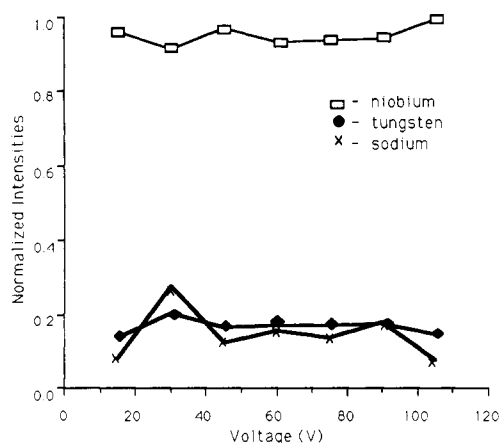


**Figure 3.** Graphed XPS data showing the trends of the niobium  $3d_{5/2}$ , tungsten  $4f_{7/2}$ , and sodium  $1s$  signals for species at the surface. Films grown at constant temperature of 35 °C to varying terminal voltages.

creased etch time (i.e., depth beneath the surface).

#### Bulk Characterization of Niobium Oxide Films.

Bulk analysis on identical sample sets was carried out on the two sample sets grown at varying temperatures. This was done at the Catholic University, Rio de Janeiro, Brazil. Figure 7 is an RBS spectrum of the niobium sample grown to 72 V at 24 °C. The region between 750 and 800 channels corresponds to the incorporated tungsten species. This region can be fitted by two clearly distinguished peaks, with the remainder of the tungsten structure being treated as one "peak". The oxide step appears between 675 and 750 channels and corresponds to the thickness of the anodic oxide layer. The metal substrate plateau extends below 675 channels. Figure 8 is an RBS spectrum of the tungsten region for the niobium sample grown to 100 V at 44 °C. In this case, the data can be fitted to five equidistant peaks. The presence of the layered structure for these sample sets was expected on the basis of previous work.<sup>15-18</sup>

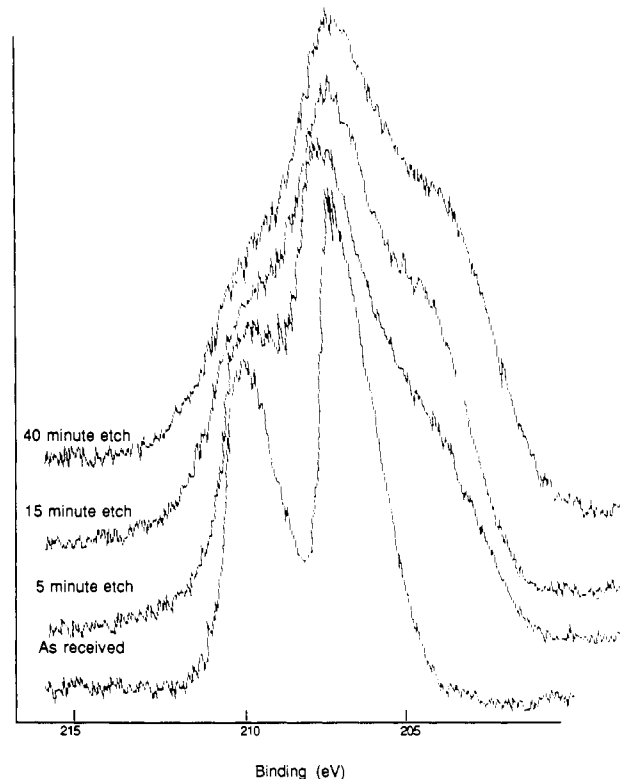


**Figure 4.** XPS of the niobium  $3d_{5/2,3/2}$  region for the sample grown at 35 °C to a terminal voltage of 30 V. Comparison of as received and after 5-, 15-, and 40-min etches. Note the reduction of niobium as indicated by the shift to lower binding energies.

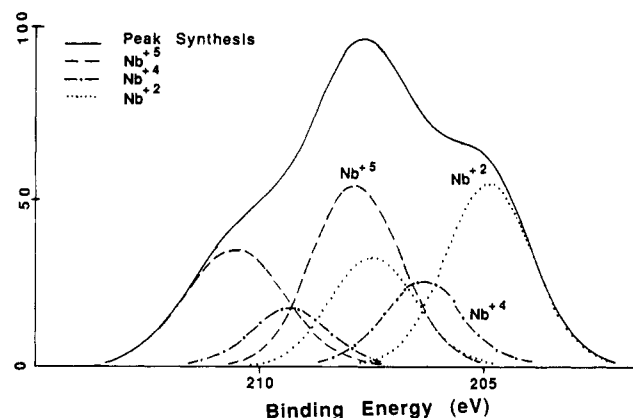


**Figure 5.** Peak synthesis of the niobium  $3d_{5/2}$  signal for the sample grown at 35 °C to a terminal voltage of 30 V after 40 min of etching. Three oxidation states of niobium (+2, +4 and +5) are present.

For each sample, the oxide layer thickness was calculated from the energies of the backscattered particles at the surface and metal/oxide interface. The energy-depth correlation is determined by an iterative process described previously.<sup>19</sup> These calculations show the average growth or anodizing ratio to be 21 Å/V. This value is consistent with values reported in other studies.<sup>20,21</sup>

The stoichiometric ratio of the oxide was also determined by using methods that have proved to be highly

(15) Barros Leite, C. V.; Baptista, G. B.; Patnaik, B. K.; Cocke, D. L.; Magnussen, N.; Murphy, O. J.; Schweikert, E. A.; Quinones, L. *J. Trace Microprobe Technol.* 1986, 4, 37.

(16) Cocke, D. L.; Kormali, S. M.; Barros Leite, C. V.; Murphy, O. J.; Schweikert, E. A.; Filpus-Luyckx, P.; Polansky, C. A.; Halverson, D. E. *J. Chem. Soc., Chem. Commun.* 1984, 1560.

(17) Cocke, D. L.; Murphy, O. J.; Kormali, S. M.; Barros Leite, C. V.; Schweikert, E. A.; Filpus-Luyckx, P.; Polansky, C.; Halverson, D. E. *J. Electrochem. Soc.* 1985, 132, 3065.

(18) Magnussen, N.; Quinones, L.; Cocke, D. L.; Schweikert, E. A.; Patnaik, B. K.; Barros Leite, C. V.; Baptista, G. B. *Thin Solid Films*, in press.

(19) Barros Leite, C. V.; Baptista, G. B.; Montenegro, E. C.; Paschoa, A. S. *J. Radioanal. Nucl. Chem.* 1987, 90, 145.

(20) Hofmann, S.; Sanz, J. M. *J. Trace Microprobe Technol.* 1982, 1, 213.

(21) Gray, K. E. *Appl. Phys. Lett.* 1975, 27, 462.

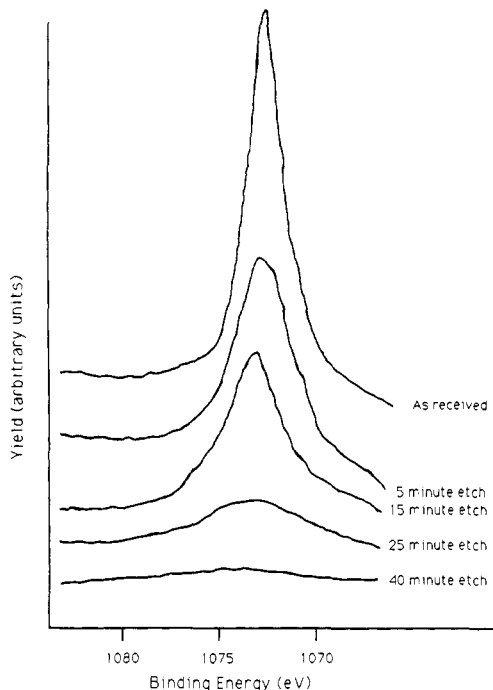


Figure 6. XPS spectra of the sodium 1s region for the sample grown at 35 °C to a terminal voltage of 30 V. Comparison of as received and after 5-, 15-, 25-, and 40-min etches.

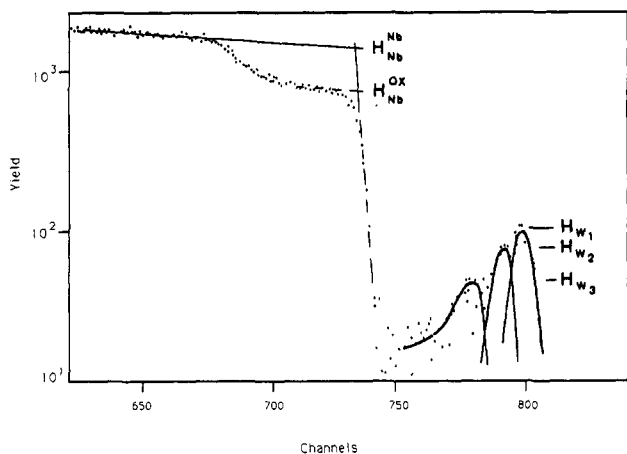


Figure 7. RBS spectrum of the niobium system grown at 24 °C to a terminal voltage of 72 V.

reliable on other anodic systems.<sup>15</sup> The stoichiometric ratio is given by the usual relation:<sup>15</sup>

$$\frac{n}{m} = \left( \frac{H_{Nb}^{Nb}}{H_{Nb}^{NbO_n}} - 1 \right) \frac{[\epsilon]_{Nb}^{Nb}}{[\epsilon]_{Nb}^O}$$

where  $H_{Nb}^{Nb}$  and  $H_{Nb}^{NbO_n}$  are the yields corresponding to the scattering of particles from niobium in the oxide layer and the pure metallic layer (extrapolated), respectively, at the surface (Figure 7). The  $[\epsilon]_{Nb}^{Nb}$  is the stopping power factor for  $\alpha$  particles scattered by niobium. The  $[\epsilon]_{Nb}^O$  is the stopping power factor of  $\alpha$  particles scattered by solid oxygen. The stopping power values used are those of Chu.<sup>22</sup> An average ratio of  $n/m = 2.0$  (10% precision), or an oxide formula of  $NbO_{2.0}$ , was calculated for the eight samples grown at varying temperatures. This is interesting since classical work<sup>14</sup> in anodically grown films would predict an average ratio of  $n/m = 2.5$ .

(22) Chu, W. K.; Mayer, J. W.; Nicolet, M. A. *Backscattering Spectrometry*; Academic Press: New York, 1978.

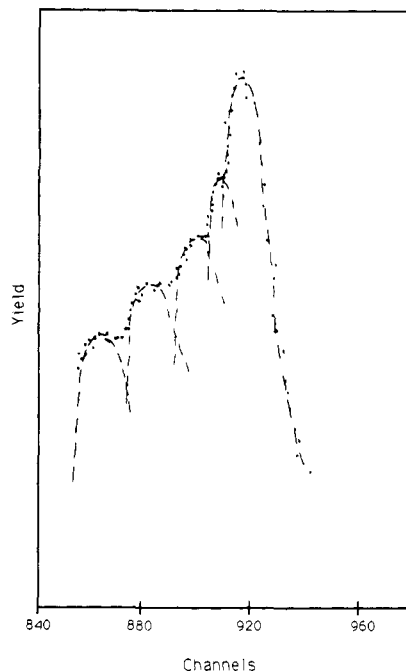


Figure 8. RBS spectrum showing the tungsten region for the sample grown at 44 °C to a terminal voltage of 100 V.

### Discussion

The stoichiometry of niobium oxide and the oxidation of niobium metal are of considerable interest, especially in the realm of superconductivity. Niobium oxide exists in three principal forms:  $Nb_2O_5$ ,  $NbO_2$ , and  $NbO$ , but several suboxides of the form  $NbO_x$  are also known and the structure of many of these have been reported.<sup>23</sup>

The stages of oxidation of niobium metal have been studied under a variety of conditions, and the results are just as varied. Some studies claim that  $NbO_2$  is the first product of oxidation, with  $Nb_2O_5$  growing at the expense of  $NbO_2$ .<sup>24,25</sup> In contrast, other studies<sup>26,27</sup> find that the existence of either  $NbO$  or  $NbO_2$  depends on the experimental growth conditions. More recent work<sup>28-30</sup> indicates that  $NbO$  forms on the niobium metal surface at room temperature and ultrahigh vacuum conditions, followed by a buildup of  $NbO_2$ . The initial  $NbO$  layer has been proposed to serve as a diffusion barrier to further oxygen penetration.<sup>31,32</sup> At higher oxygen exposures and higher temperatures, it is suggested that  $NbO_2$  begins to form and breaks up the protective layer.<sup>30</sup> Finally, at high oxygen exposures the stable  $Nb_2O_5$  forms as a thick, porous layer.

The present work adds new information to the understanding of the anodic oxidation of niobium and, in particular, the effect of anion incorporation in the growth process. The surface characteristics are examined by XPS, and these results are significant in that they show the close association of the sodium and tungsten species for all three sample sets. This trend was first reported for titanium and zirconium oxide films grown in the presence of sodium tungstate.<sup>18</sup> Normally, a sodium signal is expected to be

(23) Terao, W. *Jpn. J. Appl. Phys.* 1963, 2, 156.  
 (24) Hurlen, T. *J. Inst. Met.* 1960, 89, 273.  
 (25) Kofstad, P.; Espevik, S. *J. Electrochem. Soc.* 1966, 112, 155.  
 (26) Sheasby, J. S.; Wallwork, G. R.; Smeltzer, W. W. *J. Electrochem. Soc.* 1966, 113, 1225.  
 (27) Sheasby, J. S. *J. Electrochem. Soc.* 1968, 115, 695.  
 (28) Sanz, J. M.; Hoffmann, S. *J. Less-Common Met.* 1983, 92, 317.  
 (29) Pantel, R.; Bujor, M.; Bardolle, J. *Surf. Sci.* 1977, 62, 589.  
 (30) Lindau, I.; Spicer, W. E. *J. Appl. Phys.* 1974, 45, 3720.  
 (31) Ronay, M.; Latta, E.-E. *Phys. Rev. B* 1985, 32, 5375.  
 (32) Ronay, M.; Nordlander, P. *Phys. Rev. B* 1987, 35, 9408.

present with random intensity, indicating sodium is present in the form of a contaminant, arising from either the sodium borate buffer or the sodium tungstate salt. However, it has been noted that the sodium and tungsten species appear to be incorporated in proportional amounts into the growing film. This supports the likelihood that the two species are forming some type of reaction product during the film growth process. Also, the XPS data show an indirect relationship between the amount of niobium and the amount of sodium and tungsten present at the surface for all three cases. This indicates that the sodium and tungsten species are displacing or covering the metal oxide.

As stated earlier, XPS is very useful for determining which species are present at the surface. In addition, in many cases, it can provide information regarding the oxidation state of the species. The binding energies observed in both experiments show the niobium to be present at a binding energy of 207.3 eV. This is consistent with values reported for Nb<sub>2</sub>O<sub>5</sub> (207.4 eV),<sup>33</sup> which is the most stable form of niobium oxide in the presence of oxygen. The tungsten signal appears at 35.5 eV, which is appropriate for tungsten in the +6 state. Unfortunately, it is not possible to identify which tungsten +6 species is present since this value falls within the range of both tungsten trioxide (35–36.5 eV) and the tungstate species (35.8 eV).<sup>33</sup> At this point it would appear more likely that the tungsten is present in anion form and associated with the sodium cation.

Depth-profiling data were collected on the sample grown at 35 °C to a terminal voltage of 30 V. Figure 4 compares the niobium region of the sample as received and after periodic etching. From this plot it is apparent that as the outer Nb<sub>2</sub>O<sub>5</sub> layers are sputtered, reduced niobium oxides are created. On the basis of other work,<sup>20,34</sup> it is suggested that the initial sputtering (less than 15 min) results in a preferential sputtering of oxygen from the surface layers. Subsequently, it is expected that an equilibrium will be reached between the reduced forms of niobium. Evidence of reduction is shown in the XPS spectra as a shift of the niobium (3d<sub>5/2,3/2</sub>) peak to the right to lower binding energies. This shift is similar to that seen in the literature.<sup>20,34</sup> Hofmann and Sanz<sup>20</sup> demonstrated that a linear relationship exists between the niobium valency and the binding energy, with each shift of 1 eV corresponding to one change in the oxidation number. If this assumption is invoked for the present study, then the shift of 3 eV seen in Figure 4 would indicate that the low binding energy shoulder is caused predominantly by the presence of Nb<sup>2+</sup>. Though the signal for Nb<sup>4+</sup> is never clearly resolved in Figure 4 (due to the close proximity of the Nb<sup>5+</sup> signal), through peak synthesis it was determined (Figure 5) that Nb<sup>2+</sup> is present.

Figure 6 plots the sodium 1s signal and shows that sodium is present throughout the region where tungsten incorporation occurs. The presence of sodium deep within the film is necessary to support the close association of sodium and tungsten in precipitation layers.

At first glance it may appear that the XPS results contradict the RBS data, which predict a stoichiometry of NbO<sub>2</sub> for the entire film. However, the minimum layer analyzed (depth resolution) in RBS is approximately 175 Å for niobium oxide,<sup>15</sup> whereas for XPS the photoelectron

escape depth is approximately 20–40 Å. Thus, it is not surprising that the surface probed by XPS shows primarily Nb<sub>2</sub>O<sub>5</sub>, while the region analyzed by RBS indicates an average stoichiometry of NbO<sub>2</sub>.

As in our previous work,<sup>15–18</sup> the RBS data show multiple peaks in the tungsten region for the samples grown at varying temperatures to a terminal voltage of 72 and 100 V. This provides additional evidence for the general nature of this structure.

Each peak in the tungsten region of the spectrum represents partially overlapping tungsten layers within the niobium oxide layer. For the niobium oxide system grown to 72 V (Figure 7), two peaks can be clearly fitted. The peak structure at lower energies cannot be positively fitted because of low concentrations of the incorporated species, therefore, this entire region is treated as one "peak" for calculation purposes. The early work done on anodic oxide systems provided information on how to obtain the best fit for the peak structures observed.<sup>17</sup> This early work was done by using a 40-MeV Ar<sup>4+</sup> ion beam in the backscattering experiment, resulting in clearly resolved peaks in the tungsten region. The tungsten region of the niobium oxide films grown to 100 V at varying temperatures can be fitted with five equidistant peaks, as was seen by the example in Figure 8.

For both the 72- and 100-V experiment, the peak at highest energy (channels) corresponds to the layer closest to the oxide surface. Layers far below the surface appear at lower energies or channels. In addition, as the depth is increased, the intensity decreases, indicating that less tungsten is present in the deeper layers. This pattern of incorporation is similar to that seen previously for zirconium oxide films grown in the presence of sodium tungstate.<sup>18</sup> However, unlike that system, the amount of tungsten incorporated does not decrease with increasing terminal voltage. In the present study, the amount of tungsten incorporated at 72 V is far smaller than the amount incorporated at 100 V. All samples grown to 100 V exhibited a five-peak structure, whereas the samples grown to 72 V showed three or less peaks in the tungsten region. Another similarity with the zirconium system is that the growth times for the present study are also unaffected by the temperature of the forming solution.

In an effort to explain the layered structures observed in the RBS and the close association of the sodium and tungsten species in the XPS, a mechanism of anion incorporation was suggested<sup>18</sup> that involves what is known as the Liesegang phenomena.<sup>35</sup> Briefly, this relies on the periodic precipitation of a supersaturated species,<sup>36</sup> in this case a reaction product involving sodium and a tungsten species. This supersaturated species forms precipitation bands within the forming oxide layer. Under the effect of an electric field, it has been shown<sup>37</sup> that these bands become evenly spaced with respect to the origin (metal oxide–solution interface). This is in agreement with the results obtained from the RBS data, where for all systems examined, evenly spaced banding has been observed.

### Conclusions

The following conclusions are significant in this study:

The XPS data show a strong, direct relationship between the sodium and tungsten species at the surface (Figures 1–3). The surface is composed of the highly stable Nb<sub>2</sub>O<sub>5</sub>, as expected. The binding energy values for the tungsten species are in agreement with the presence of an

(33) Riggs, W. M.; Davis, L. E.; Moulder, J. F.; Murlenberg, G. F. *Handbook of X-ray Photoelectron Spectroscopy*; Physical Electronics Ind.: Eden Prairie, MN, 1979.

(34) Jouve, J.; Belkacem, Y.; Severac, C. *Thin Solid Films* 1986, 139, 67.

(35) Liesegang, R. E. *Photogr. Archiv.* 1986, 21, 221.

(36) Ostwald, W. Z. *Phys. Chem.* 1897, 23, 365.

(37) Ortoleva, P. *Theoretical Chemistry*; Academic: New York, 1978.

anionic species. This supports the possibility of a reaction product formed between sodium and the tungsten species.

Depth profiling shows (Figures 4 and 5) the reduction of  $\text{Nb}_2\text{O}_5$  to  $\text{Nb}^{4+}$  and  $\text{Nb}^{2+}$ . Preferential sputtering leads to the presence of a steady-state mixture of niobium oxidation states. The presence of sodium is also confirmed (Figure 6) by depth profiling. This is expected if sodium and tungsten are associated in the form of a precipitation product.

Calculations based on the RBS data suggest an average stoichiometric formula of  $\text{NbO}_2$  for the oxide layer. This is unexpected based on other studies of anodically grown niobium films which predict the presence of  $\text{Nb}_2\text{O}_5$ . Also, the RBS data (Figures 7 and 8) show evenly spaced precipitation bands, as would be expected for a precipitation reaction occurring under the influence of an electric field. In addition, it was noted that increased voltage (100 V as compared to 72 V) allowed the formation of a more extensive layering structure (five peaks as opposed to three peaks) within the oxide film. This is useful for those

materials where maximum incorporation of anions would be beneficial.

The anodic oxidation of niobium and the incorporation of anions into forming anodic films are important areas of research. With increased understanding of how these processes operate, steps can be made to control and adapt these processes to our needs.

**Acknowledgment.** We are grateful for the editorial assistance of Eileen Perry and Lorraine Puckhaber in the preparation of the manuscript. In addition, the technical assistance given by Karl Balke and Eric Halverson in the collection of data was highly appreciated. This work was supported by grants from the Board of Regents at Texas A&M University, the Texas Advanced Technology Research Program (TATRP), the National Science Foundation (Grant INT 8602288), and the Conselho Nacional de Desenvolvimento Científico e Tecnológico (CNPq).

**Registry No.** Nb, 7440-03-1;  $\text{Nb}_2\text{O}_5$ , 1313-96-8; sodium tungstate, 11120-01-7.

## Electronic Transmission Coefficient as a Tool for the Analysis of the Effect of Impurities and Defects on the Electronic Structure of Polymers

Philippe Sautet,\* Odile Eisenstein, and Enric Canadell

Laboratoire de Chimie Théorique,<sup>†</sup> Bât 490, Université de Paris—Sud, 91405 Orsay Cedex, France

Received September 6, 1988

The effect of impurities and defects on the electronic structure of some polymeric chains has been approached by considering a model infinite chain  $\cdots\text{AAAABAAAA}\cdots$ , where B is an impurity or defect embedded in an infinite chain  $\cdots\text{AAAAA}\cdots$ . The transmission coefficient  $t(E)$  and differential density of states  $\Delta\text{DOS}(E)$  curves have been used to characterize the different types of interactions between an impurity/defect level and an energy band. When the energy band can interact with more than one level of the impurity/defect, interference effects have to be considered. A rule to predict the constructive/destructive nature of these interferences is given. The use of the transmission coefficient as an analytical tool and the connection with the usual orbital interaction analysis of the electronic structure of molecules and solids are illustrated. The effect of several C=X impurities (X = O, S,  $\text{CH}_2$ ) and  $\text{sp}^3$  defects as well as donor and acceptor pendant groups on the electronic structure of polyacetylene chains has been considered.

### 1. Introduction

Impurities and defects have a strong influence on the electronic structure of polymeric materials. Hence, several theoretical approaches have been recently developed<sup>1</sup> with the aim of understanding the consequences of this rupture of translational invariance. Important tools to analyze the phenomenon, like the density of states or the charge-bond order matrix for several imperfect polymers have thus been evaluated.<sup>1</sup> Sometimes, the problem has been faced from a different methodological perspective, by using standard quantum chemical methods to perform calculations on discrete molecular species aiming to represent the local

effect of such impurities.<sup>2-5</sup> Although both approaches have been very important in providing a basis for the understanding of the chemistry of these imperfect polymers, they seem to be less well suited to face one of the most exciting problems in the field, i.e., the control of

(1) For some leading references see: (a) Ladik, J.; Seel, M. *Phys. Rev. B* 1976, 13, 5338. (b) Del Re, G.; Ladik, J. *Chem. Phys.* 1980, 49, 321. (c) Seel, M.; Ladik, J. *Phys. Rev. B* 1985, 32, 5124. (d) Seel, M.; Del Re, G.; Ladik, J. *J. Comp. Chem.* 1982, 3, 451. (e) Seel, M. *Int. J. Quantum Chem.* 1984, 26, 753. (f) Gies, M.; Seel, M.; Ladik, J. *J. Mol. Struct. (THEOCHEM)* 1987, 150, 267. (g) Hennico, G.; Delhalle, J.; André, J.-M.; Seel, M.; Ladik, J. *Solid State Commun.* 1987, 64, 1257. (h) Biczio, G. *Can. J. Chem.* 1985, 63, 1992, and references therein. (i) The case of an impurity B embedded in an infinite linear chain  $\cdots\text{AABAA}\cdots$  has also been briefly considered by using the moments method: Burdett, J. K.; Lee, S.; Sha, W. C. *Croat. Chem. Acta* 1984, 57, 1193.

(2) Jeyadev, S.; Conwell, E. M. *Phys. Rev. B* 1988, 37, 8262.

(3) Tanaka, S.; Yamanaka, S.; Koike, T.; Yamabe, S. *Phys. Rev. B* 1985, 32, 2731.

(4) Surjan, P. R.; Kuzmany, H. *Phys. Rev. B* 1986, 33, 2615.

(5) Navarrete, J. T. L.; Zerbi, G. *Solid State Commun.* 1987, 64, 1183.

\* To whom correspondence should be addressed at Institut de Recherche sur la Catalyse, 2 Av. Albert Einstein, 69626 Villeurbanne Cedex, France, or Laboratoire de Chimie Théorique, Ecole Normale Supérieure de Lyon, 69364 Lyon Cedex 07, France.

<sup>†</sup> The Laboratoire de Chimie Théorique is associated with the CNRS (UA 506) and is a member of ICMO and IPCM (Orsay).